第 34 卷第 10 期
2018 年 10 月

无 机 化 学 学 报
CHINESE JOURNAL OF INORGANIC CHEMISTRY

Vol.34 No.10
1929-1935

柱状 Co_3O_4 催化剂的乏风催化燃烧性能

牛汝月[1] 刘鹏程[1] 李 威[1] 王 爽*,[1,2] 李晋平*,[1]

([1]气体能源高效清洁利用山西省重点实验室,太原 030024)

([2]太原理工大学环境科学与工程学院,晋中 030600)

摘要:通过两步法成功合成了由纳米粒子组装成的柱状 Co_3O_4。第一步是通过简单的冷凝回流法合成柱状 $CoC_2O_4·2H_2O$。第二步将所制备的柱状 $CoC_2O_4·2H_2O$ 在 350 ℃下煅烧 2 h,使其分解形成 Co_3O_4 而不破坏原始形貌。通过粉末 X 射线衍射(PXRD),X 射线光电子能谱(XPS),氮气吸附-脱附,扫描电镜(SEM),高分辨率透射电子显微镜(HRTEM)和 H_2 程序升温还原(H_2-TPR)表征柱状 Co_3O_4 的物化性质。结果表明,柱状 Co_3O_4 对乏风甲烷燃烧的催化活性远远高于商业 Co_3O_4。柱状 Co_3O_4 优异的催化性能可能归因于其表面较高的 Co^{3+} 含量,较高的表面吸附氧和大量暴露的{111}晶面族。

关键词:工业催化;金属氧化物催化剂;催化活性;乏风甲烷

中图分类号:O643.36 **文献标识码**:A **文章编号**:1001-4861(2018)10-1929-07

DOI:10.11862/CJIC.2018.223

Catalytic Combustion of Ventilation Air Methane over Co_3O_4 Rectangular Prism

NIU Ru-Yue[1] LIU Peng-Cheng[1] LI Wei[1] WANG Shuang*,[1,2] LI Jin-Ping*,[1]

([1]*Shanxi Key Laboratory of Gas Energy Efficient and Clean Utilization, Taiyuan* 030024, *China*)

([2]*College of Environmental Science and Engineering, Taiyuan University of Technology, Jinzhong, Shanxi* 030600, *China*)

Abstract: The Co_3O_4 rectangular prism assembled by nanoparticles has been successfully fabricated via a two-step method. The first step involves the synthesis of $CoC_2O_4·2H_2O$ rectangular prism by a simple condensing reflux method. The second step includes the calcination of the as-prepared $CoC_2O_4·2H_2O$ rectangular prism at 350 ℃ for 2 h, causing its decomposition to form Co_3O_4 rectangular prism without destructing of the original morphology. The mechanical properties were characterized by powder X-ray diffraction (PXRD), X-ray photoelectron spectroscopy (XPS), nitrogen adsorption-desorption, scanning electron microscopy (SEM), high-resolution transmission electron microscopy (HRTEM), and H_2 temperature-programmed reduction (H_2-TPR). The results showed that the catalytic activity of Co_3O_4 rectangular prism for the combustion of ventilation air methane was higher than that of commercial Co_3O_4. The superior catalytic performance could be attributed to the high surface Co^{3+} content, high surface adsorbed oxygen content, and exposing the {111} planes.

Keywords: industrial catalysis; metal oxide catalyst; catalytic activity; ventilation air methane

0 Introduction

As is known, methane is difficult to be oxidized due to the strongest C-H bond among hydrocarbons, however, it has been studied extensively over the past decades, and the catalytic combustion is still a challenging technology that can convert methane into carbon dioxide and water at relatively low temperature [1-4]. Especially, ventilation air methane (VAM) is much more difficult to be oxidized for its low concentration (0.1%~

收稿日期:2018-05-30。收修改稿日期:2018-07-12。

国家自然科学基金面上(No.21671147),山西省煤层气联合基金(No.2016012004)和高等学校科技创新项目资助。

*通信联系人。E-mail:wangshuang@tyut.edu.cn,jpli211@hotmail.com

1.0% (*V*/*V*)) and fast flow rate[5]. Up to now, about 60%~70% methane is emitted to the atmosphere through VAM all over the world, particularly, in China, about 85%~90% of the total coal mine methane emissions mainly comes from VAM each year[6-7]. Moreover, the warming potential of methane is higher than that of carbon dioxide. Therefore, the efforts to remove methane from VAM and limit the emission of toxic gases become rather important[8].

Accordingly, catalysts for methane combustion undergo very demanding conditions: they must resist thermal, mechanical shocks and exhibit high activity. Noble metal-based catalysts, such as supported Pd and Pt catalysts, are well-known to be high activity at low temperature. Unfortunately, they are limited in industrial applications due to their high cost and low thermal stability[9-11]. Alternatively, oxide catalysts such as perovskites, hexaaluminates and transition metal oxides catalysts are the promising combustion catalysts with a low cost and relatively high thermal stability in methane combustion[12-15]. Compared to other oxide catalysts, cobalt oxide (Co_3O_4) is regarded as the most efficient catalyst, and many researchers identified that the activity for methane combustion follows the order: Co_3O_4 > CuO > NiO > Fe_2O_3 > Mn_2O_3 > Cr_2O_3[16-18].

Generally, the morphologies and the crystal planes of Co_3O_4 nanocrystals have promoting performances in methane combustion. Chen et al.[19] reported that the Co_3O_4 catalysts containing {111} planes exhibit the higher catalytic activity than the {100} planes for the methane combustion, which confirms the effect of crystal planes on the catalytic performance. Moreover, some researches show that the high Co^{3+}/Co^{2+} ratio is favorable to the methane combustion, because it can facilitate desorption of oxygen and in turn assist methane combustion[20-21]. Furthermore, the adsorbed oxygen species play an important role in catalytic oxidation reactions[22-24]. For example, Fei et al.[25] suggested that the Co_3O_4 nanotubes have higher catalytic activity than the Co_3O_4 nanoparticles in the methane combustion, because the nanotubes Co_3O_4 possess much more adsorbed oxygen.

In the current work, a Co_3O_4 rectangular prism catalyst was prepared by a two-step method, and its catalytic activity was evaluated by the temperature of methane combustion in VAM. The relationship between the structure and catalytic performance of the above-mentioned catalyst is well studied based on plenty of characterizations such as PXRD, SEM, HRTEM, N_2 adsorption-desorption, H_2-TPR, and XPS.

1 Experimental

1.1 Materials

All the reagents were obtained from commercial sources and used without further purification. Cobalt(Ⅱ) acetate tetrahydrate (99.5%) was purchased from Sinopharm Chemical Reagent Co., Ltd. Oxalic acid (99.0%) was purchased from Tianjin Chemical Reagent Co., Ltd. Hexamethylenetetramine (99.0%) was purchased from Tianjin Beichen Founder Reagent Factory. All used gases were high pure gases (99.99%).

1.2 Preparation of the catalysts

In a typical synthesis procedure, 20 mmol of Cobalt (Ⅱ) acetate tetrahydrate was dissolved in 100 mL of distilled water at 40 ℃. Then 10 mL of an aqueous solution containing 20 mmol of hexamethylenetetramine and 4 mmol of oxalic acid was added dropwise under stirring within two minutes. The pink turbidity solution was refluxed at 95 ℃ for 6 h and a light pink Co-based precursor was obtained. The Co_3O_4 was made by heating the precursor at 350 ℃ in air for 2 h.

1.3 Characterization of the catalyst

The phase purity and crystal structure of the catalysts were examined on a Rigaku Mini Flex Ⅱ benchtop X-ray diffractometer using Cu $K\alpha$ radiation (30 kV, 15 mA, λ=0.154 18 nm) in the 2θ range of 10°~80° with a step size of 0.01° and a scanning rate of 8°·min^{-1}.

Morphologies of the samples were observed by SEM (Hitachi, SU8010, 3 kV). The HRTEM measurement was carried out with FEI Tecnai G2 F20 S-Twin equipment operated at an accelerating voltage of 200 kV. The catalyst powder was ultrasonically dispersed in ethanol and dropped onto a copper grid coated with amorphous carbon film, then dried in air.

The Brunauer-Emmett-Teller (BET) surface area and pore size distribution of the catalyst were measured with a Micromeritics TriStar Ⅱ 3020 instrument using adsorption of N_2 at 77 K. Before each adsorption experiment, the catalyst was heated at 200 ℃ under vacuum for 3 h.

Barrett-Joyner-Halenda (BJH) method was used to calculate the pore size distribution from desorption branch of the isotherm.

The X-ray photoelectron spectroscopy (XPS) test was performed on an ESCALAB 220i-XL spectrometer by using Al $K\alpha$ (1 486.6 eV) as the X-ray source. The equipment base pressure was 3×10^{-5} Pa, and the sample was characterized at room temperature. Detailed spectra were recorded for the region of Co2*p* and O1*s* photoelectrons with a 0.1 eV step. Analysis was performed by the XPS Peak Fit software, and charging effects were corrected by adjusting binding energy (B.E.) of C1*s* (284.6 eV).

The H_2-temperature programmed reduction (H_2-TPR) was analyzed with a Micromeritics AutoChem Ⅱ 2920 instrument. Prior to H_2-TPR experiment, 50 mg catalyst was purged in flowing Ar at 200 ℃ for 1 h with a total flow rate of 30 mL·min^{-1}, then cooled down to 50 ℃ in Ar flow. The reduction process was carried out in the temperature range of 50~900 ℃ in H_2/Ar (V_{H_2}/V_{Ar}= 10%, 30 mL·min^{-1}). The hydrogen consumption was estimated from the area under the peak after taking the thermal conductivity detector response into consideration. Calibration of thermal conductivity detector (TCD) signal has been done with an Ag_2O standard (Merck, reagent grade). The data processing has been done by using Origin Pro 8.0 program, which allows the deconvolution of the temperature-programmed reduction (TPR) peaks in well-defined Gaussian-shaped components.

1.4 Catalytic activity measurement

The methane combustion on Co_3O_4 rectangular prism catalyst was carried out at atmospheric pressure in a conventional flow system using a fixed-bed quartz micro-reactor (length=400 mm, inner diameter=6 mm). A gas mixture consisted of CH_4, O_2 and N_2 (V_{CH_4}:V_{O_2}:V_{N_2}=1:20:79) was introduced into the quartz micro-reactor at a total flow rate of 40 mL·g^{-1}·h^{-1} corresponding to a gas hourly space velocity (GHSV) of 16 000 mL·g^{-1}·h^{-1}. When GHSV changed from 16 000 to 112 500 mL·g^{-1}·h^{-1}, the total flow rate was varied from 40 to 150 mL·g^{-1}·h^{-1}. According to different GHSVs, 80~150 mg of catalysts (20~40 mesh) were loaded in the quartz tube micro-reactor, respectively. Prior to each measurement, the catalyst was pretreated at 200 ℃ for 1 h with a nitrogen flow of 30 mL·min^{-1}. Activity data were obtained at steady state condition from 200 to 450 ℃ while increasing the temperature by 50 ℃.The effluent gases were analyzed online with a gas chromatograph (ZHONGKEHUIFEN GC-6890A) equipped with a TDX-01 column and a thermal conductivity detector. The methane conversion (X_{CH_4}) was calculated according to the following equation: $X_{CH_4}=(X_0-X_T)/X_0\times100\%$, where X_0 refers to the volumetric concentration of methane in the feed and X_T corresponds to the concentration of methane at the given temperature. In all tests, CO_2 and H_2O were the only detected products in the exhaust stream during reaction, and CO was not found in the effluent gases, implying the conversion of methane to carbon dioxide. For comparison, commercial Co_3O_4 was also investigated.

2 Results and discussion

2.1 Structural and morphological analysis

Fig.1a presents the PXRD patterns of as-prepared $CoC_2O_4\cdot2H_2O$ precursors. The presence of peaks at 2θ= 18.7°, 22.7°, 30.1°, 35.0°, 37.6°, 40.4°, 43.3°, 47.3°, 48.4°, and 51.1° could be assigned to the (202), (004), (400), (022), (206), (315), (224), (602), (026) and (130) planes of $CoC_2O_4\cdot2H_2O$ (PDF No.48-1068). In the Fig. 1b, the diffraction peaks of Co_3O_4 rectangular prism at 19.0°, 31.2°, 36.6°, 38.5°, 44.8°, 55.7°, 59.4° and 65.3° could be assigned to the (111), (220), (311), (222), (400), (422), (511) and (440) planes of the spinel phase Co_3O_4 (PDF No.42-1467). In the case of the Co_3O_4 sample, no other peaks can be detected for impurities, which indicate that the sample consists of pure Co_3O_4 phase.

In order to have a better understanding of the morphological and structural, a detailed microscopy investigation by SEM and high-resolution analysis are performed on both $CoC_2O_4\cdot2H_2O$ precursors and Co_3O_4 catalysts. Fig.2 displays SEM imags of the as-prepared $CoC_2O_4\cdot2H_2O$ at 95 ℃ and the corresponding Co_3O_4 products after calcination. As shown in Fig.2a, most $CoC_2O_4\cdot2H_2O$ are uniform rectangular prisms with smooth surfaces, and the size distribution is in the range of 2~5 μm (Fig.2b). Fig.2(c,d) show the SEM images of the prepared Co_3O_4 catalysts after calcination at 350 ℃. It is found that most of the Co_3O_4 catalysts well maintain the

rectangular prism shape. Fig.3 shows the HRTEM images of Co_3O_4 catalysts. Seen in Fig.3a, the Co_3O_4 catalyst is formed by the accumulation of small particles of 10~20 nm, ultrasonication results in the breakdown of rectangular prisms into nanoparticles. Their lattice fringes are clear (Fig.3b), which are attributed to (220) planes with a lattice space of 0.278 nm. The dominant exposed plane of Co_3O_4 rectangular prisms is {111} planes, which is the plane normal to the set of (220) planes.

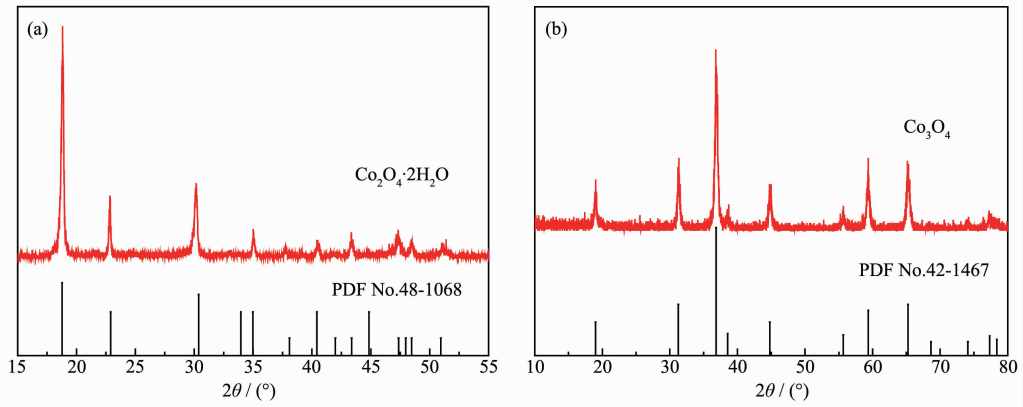

Fig.1 PXRD patterns of $CoC_2O_4 \cdot H_2O$ precursors (a) and Co_3O_4 catalysts (b)

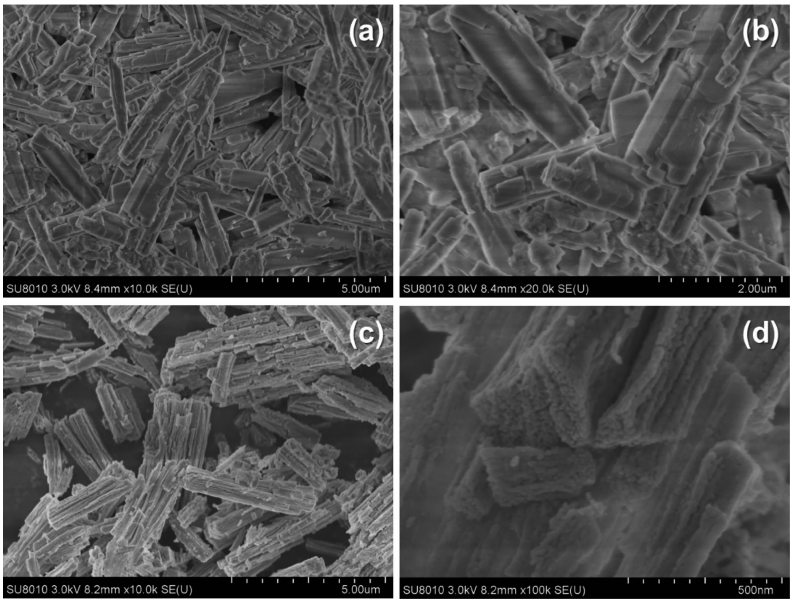

Fig.2 SEM images of (a, b) $CoC_2O_4 \cdot H_2O$ precursors and (c, d) Co_3O_4 catalysts

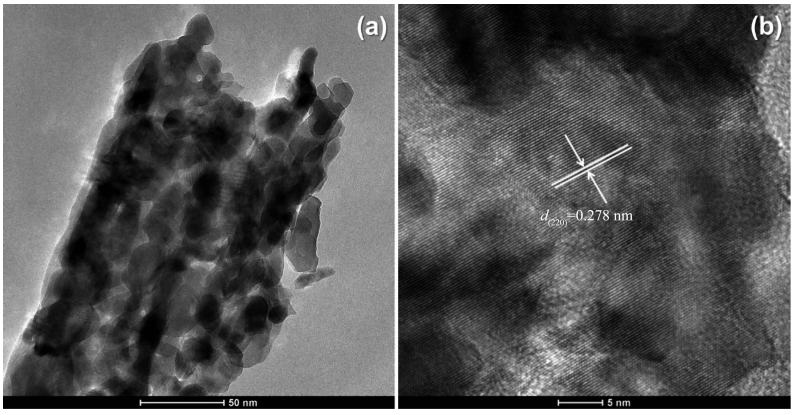

Fig.3 HRTEM images for Co_3O_4 catalysts

2.2 Specific surface area and pore diameter distribution

To further investigate the specific surface areas and the porous nature of the $CoC_2O_4\cdot 2H_2O$ precursors and Co_3O_4 catalysts, Nitrogen adsorption-desorption isotherms of the two samples are shown in Fig.4, and the insets illustrate the corresponding Barrett-Joyner-Halenda (BJH) pore size distribution plots. For Co_3O_4 catalysts, nitrogen adsorption experiment has given a typical type-Ⅳ isotherm with a distinct hysteresis loop observed in the relative pressure (P/P_0) range of 0.7~1.0, which is the characteristic of mesoporous materials. The BET surface area for the $CoC_2O_4\cdot 2H_2O$ precursors and Co_3O_4 catalysts are found to be about 4 and 45 $m^2\cdot g^{-1}$, respectively. The increase of BET surface area may result from the decomposition of the $CoC_2O_4\cdot 2H_2O$ precursors. Moreover, the BET surface area of the commercial Co_3O_4 catalyst is measured to be 1 $m^2\cdot g^{-1}$. According to the BJH plot calculated from the nitrogen isotherm, the average pore diameter of Co_3O_4 catalysts is about 14 nm, which indicated that the sample contains mesoscale pores.

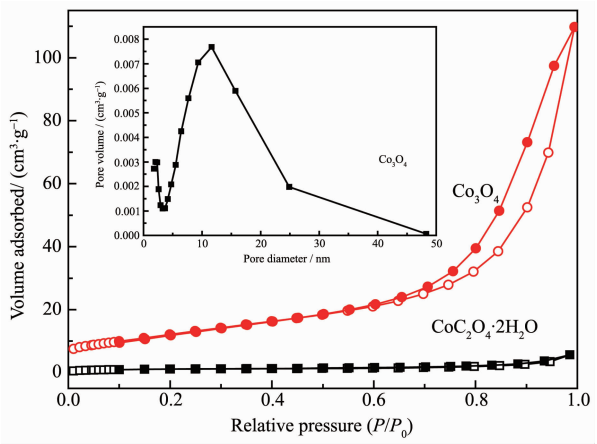

Fig.4　N_2 adsorption-desorption isotherms of Co_3O_4 catalysts and $CoC_2O_4\cdot H_2O$ precursors, and pore diameter distribution (inset) of Co_3O_4 catalysts

2.3 X-ray photoelectron spectroscopy (XPS)

XPS analysis was performed in order to gain the binding energy and the percentages of surface atoms. O1*s* and Co2*p* photoelectron spectra for the rectangular prism Co_3O_4 are shown in Fig.5. As indicated in Fig.5a, three peaks have been observed. The peak at ~529.7 eV (O^{2-}) is attributed to lattice oxygen species (O_{lat}) of the catalyst. And the peaks at ~531.3 (O^-) and ~533.0 eV (O_2^-) are attributed to the adsorption oxygen species (O_{ads})[26]. According to literatures, higher relative concentration ratio of O_{lat}/O_{ads} is previously found to be preferable for methane combustion. The ratio of the peak intensities of the surface-adsorbed oxygen species to lattice oxygen is 1.24, thus high activity for methane combustion can be obtained[27-28].

Two sharp peaks at 795.2 and 780.0 eV correspond to the Co2$p_{1/2}$ and Co2$p_{3/2}$ spin-orbit-split doublet peak of Co_3O_4 spinel, respectively. There is an energy difference of approximately 15.2 eV between them. The same chemical information can be obtained by analyzing the Co2$p_{1/2}$ and Co2$p_{3/2}$ spectra. Therefore, only Co2$p_{3/2}$ peaks in Fig.5b are fitted and de-convoluted into two peaks at 781.8 and 779.8 eV, which are attributed to Co^{2+} and Co^{3+}[28-29], respectively. Co_3O_4, containing a Co^{3+}/Co^{2+} couple, is favorable to methane combustion. Moreover, the main oxidation state of Co in the Co_3O_4 rectangular prism is Co^{3+} (the ratio of the peak intensities of Co^{3+} to Co^{2+} is 2.87), accordingly, higher oxidation state of Co species

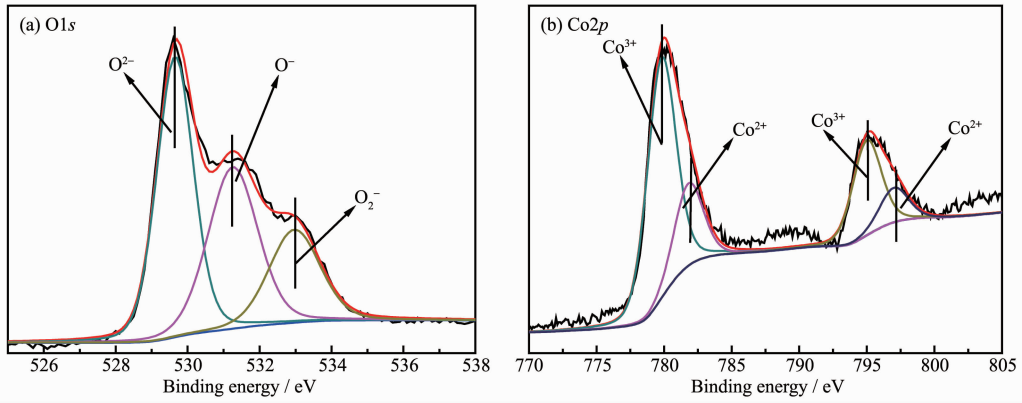

Fig.5　XPS spectra of O1**s** (a) and Co2*p* (b) for Co_3O_4 catalysts

was previously found to be preferable for oxidation reactions over the Co containing catalysts[19,30].

2.4 H_2 temperature-programmed reduction (H_2-TPR)

To investigate the reducibility of the Co species in Co_3O_4 rectangular prism and commercial Co_3O_4 catalysts, H_2-TPR experiments are carried out. The reduction profiles of the samples have been displayed in Fig.6. In this case, the Co_3O_4 rectangular prism contains two reduction peaks, the first peak is at 256 ℃, which is associated with the reduction of Co_3O_4 to CoO, and the second broad peak at 351 ℃ is correspond to the reduction of CoO to Co. However, the commercial Co_3O_4 catalysts have a wide reduction peak centered at 460 ℃. The results show that the performance of Co_3O_4 rectangular prism is better than that of commercial Co_3O_4 catalysts. Accordingly, the same oxide species, which has the lower reduction temperature, owing the easier activation of bond metal-oxygen (Co-O)[31-32].

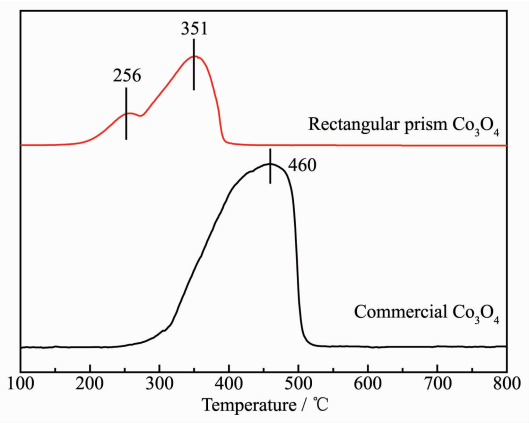

Fig.6 H_2-TPR profiles of Co_3O_4 rectangular prism and commercial Co_3O_4 catalysts

2.5 Catalytic performance for methane oxidation

The activity in methane complete oxidation was expressed in terms of methane conversion with respect to the reaction temperature for Co_3O_4. Accordingly, the catalytic activity of methane oxidation is evaluated by the light-off temperature ($T_{10\%}$), the half-conversion temperature ($T_{50\%}$) and the total conversion temperature ($T_{90\%}$), representing the temperature of methane conversions at 10%, 50% and 90%, respectively. The $T_{10\%}$, $T_{50\%}$ and $T_{90\%}$ over the rectangular prism Co_3O_4 catalyst are 236, 322 and 428 ℃ at 16 000 $mL\cdot g^{-1}\cdot h^{-1}$, respectively (Fig. 7a). However, the $T_{10\%}$ over commercial Co_3O_4 catalyst is 378 ℃, in addition, the highest methane conversion merely reached to 18.06% at 450 ℃. Moreover, the methane conversion over the rectangular prism Co_3O_4 catalyst increased with increasing temperature from 200 ~450 ℃. To convert low-concentration methane effectively by catalytic oxidation in practical application, GHSV is a critical parameter. Thus, the effects of GHSVs on methane conversion over the Co_3O_4 rectangular prism catalyst were studied. A general change is observed from Fig.7a, that is, methane conversion rates decrease as increasing GHSVs. When the GHSVs are 30 000, 60 000, 90 000 and 112 500 $mL\cdot g^{-1}\cdot h^{-1}$, the methane conversions are decreased 4.16%, 8.54%, 15.89% and 20.85% compared to 16 000 $mL\cdot g^{-1}\cdot h^{-1}$ at 450 ℃, respectively. In general, a high GHSV has provided a short residence time and frequent contacts between catalyst and reaction gases, which leads to the decrease in the methane conversions. This result displays that enough contact time is necessary for enhancing the catalytic activity. As seen in Fig.7b, the catalytic stability of the rectangular

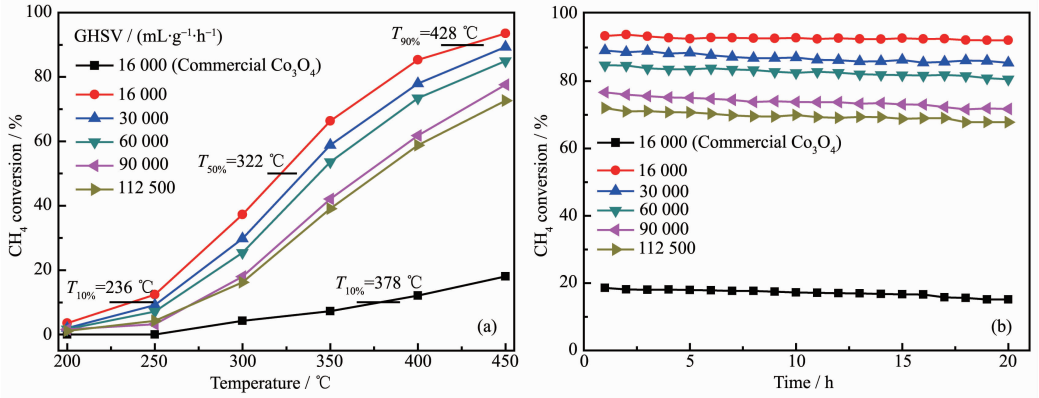

Fig.7 (a) Methane conversion curves of Co_3O_4 catalysts and commercial Co_3O_4 catalysts; (b) Long-term stability of samples at 450 ℃ under different GHSVs conditions

prism Co_3O_4 catalyst was examined at different GHSVs. After the samples were operated at 450 ℃ for 20 h under different GHSVs, the methane conversion rates only have slight decreases. For comparison, when the GHSV was 16 000 mL·g^{-1}·h^{-1}, the catalytic stability of the commercial Co_3O_4 catalyst was tested. It can be seen that the methane conversion rates keep at approximately 16% within running stable for 20 h.

3 Conclusions

In summary, a novel Co_3O_4 rectangular prism with excellent activity and good stability towards the methane combustion has been synthesized through a two-steps method. The superior catalytic activity can be attributed to the following reasons: firstly, the Co_3O_4 rectangular prism dominantly exposed the {111} crystal planes, which confirmed the effect of crystal planes on the methane combustion performance; Secondly, high surface Co^{3+} content and high content surface adsorbed oxygen both play crucial roles in the methane catalytic oxidation. Owing to its simplicity of synthesis, low cost and excellent methane combustion performance, the novel Co_3O_4 rectangular prism could be a very important and promising heterogeneous catalyst.

Acknowledgements: The authors acknowledge the financial support of the Natural Science Foundation of China (Grant No.21671147), Scientific and Technologial Innovation Programs of Higher Education Institutions in Shanxi, State Key Laboratory of Coal and CBM Co-mining.

References:

[1] O′malley A, Hodnett B K. *Catal. Today*, **1999**,**54**(1):31-38
[2] REN Xiao-Guang(任晓光), GE Xiu-Tao(葛秀涛). *Chinese J. Inorg. Chem.*(无机化学学报), **2012**,**28**(4):823-828
[3] Kirchnerova J, Alifanti M, Delmon B. *Appl. Catal., A*, **2002**, **231**(1/2):65-80
[4] CHEN Yong-Dong(陈永东), ZHU Yi(朱艺), WANG Jian-Li (王健礼), et al. *Chinese J. Inorg. Chem.*(无机化学学报), **2009**,**25**(10):1771-1778
[5] Guo T Y, Du J P, Wu J T, et al. *Chem. Eng. J.*, **2016**,**306**: 745-753
[6] Ouyang S, Xu S, Song N, et al. *Fuel*, **2013**,**113**:420-425
[7] Cheng Y P, Wang L, Zhang X L. *Int. J. Greenhouse Gas Control*, **2011**,**5**(1):157-166
[8] Guo T Y, Du J P, Li J P. *J. Mater. Sci.*, **2016**,**51**(24):10917-10925
[9] Lovón-Quintana J J, Santos J B O, Lovón A S P, et al. *J. Mol. Catal. A*: *Chem.*, **2016**,**411**:117-127
[10]Ruiz J A C, Oliveira E C, Fraga M A, et al. *Catal. Commun.*, **2012**,**25**:1-6
[11]Chen C, Yeh Y H, Cargnello M, et al. *ACS Catal.*, **2014**,**4** (11):3902-3909
[12]Cao X X, Zhou R, Rui N, et al. *Catal. Today*, **2017**,**297**:219 -227
[13]MIU Jian-Wen(缪建文), FAN Yi-Ning(范以宁), JIN Yong-Shu(金永漱), et al. *Chinese J. Inorg. Chem.*(无机化学学报), **2003**,**19**(12):1361-1365
[14]Hu R S, Ding R R, Chen J, et al. *Catal. Commun.*, **2012**,**21**: 38-41
[15]ZHENG Jian-Dong(郑建东), GE Xiu-Tao(葛秀涛). *Chinese J. Inorg. Chem.*(无机化学学报), **2013**,**29**(6):1307-1311
[16]Xu X L, Han H, Liu J J, et al. *J. Rare Earths*, **2014**,**32**(2): 159-169
[17]Zavyalova U, Scholz P, Ondruschka B. *Appl. Catal., A*, **2007**,**323**:226-233
[18]Hu L H, Peng Q, Li Y D. *J. Am. Chem. Soc*., **2008**,**130**(48): 16136-16137
[19]Chen Z P, Wang S, Liu W G, et al. *Appl. Catal., A*, **2016**, **525**:94-102
[20]Zou G C, Chen M X, Shangguan W F. *Catal. Commun.*, **2014**,**51**:68-71
[21]Wang Q, Peng Y, Fu J, et al. *Appl. Catal., B*, **2015**,**168**:42-50
[22]Chen Z P, Wang S, Ding Y, et al. *Appl. Catal., A*, **2017**, **532**:95-104
[23]Wang F G, Zhang L J, Xu L L, et al. *Fuel*, **2017**,**203**:419-429
[24]Huang H, Dai Q G, Wang X Y. *Appl. Catal., B*, **2014**,**158**: 96-105
[25]Fei Z Y, He S C, Li L, et al. *Chem. Commun.*, **2012**,**48**(6): 853-855
[26]Yang N T, Ni S L, Sun Y H, et al. *Mol. Catal.*, **2018**,**452**: 28-35
[27]Petitto S C, Marsh E M, Carson G A, et al. *J. Mol. Catal., A*, **2008**,**281**(1/2):49-58
[28]Wei Y C, Ren X, Ma H M, et al. *Chem. Commun.*, **2018**,**54** (12):1533-1536
[29]Yang H, Yang W H, Lv K L, et al. *Microporous Mesoporous Mater.*, **2018**,**255**:36-43
[30]Li Y, Shen W J. *Chem. Soc. Rev.*, **2014**,**43**(5):1543-1574
[31]Zhu Z Z, Lu G Z, Zhang Z G, et al. *ACS Catal.*, **2013**,**3**(6): 1154-1164
[32]Yan Q Y, Li X Y, Zhao Q D, et al. *J. Hazard. Mater.*, **2012**, **209**:385-391